Acoustics 2008
Geelong, Victoria, Australia 24 to 26 November 2008

Acoustics and Sustainability:

How should acoustics adapt to meet future demands?

The Design of a Constrained layer Damping Solution for Rail Car Brake Squeal

Graham Brown, Ross Emslie, David Hanson Paul Walsh, Steve Grobler, Norm Broner

Sinclair Knight Merz, Australia

ABSTRACT

Brake squeal relating to the application of tread block brakes on rail cars can generate significant noise annoyance issues and presents a challenging problem due to the associated technical complexities as well as inherent design constraints. In this paper the phenomenon of brake squeal occurring on a rail vehicle is investigated using experimental techniques. The operational vibration response of the brake head is examined as is the modal characteristics of both the brake head and the wheel. A combination of analytical and finite element methods is then used to design a constrained layer damping treatment for the rail wheel to reduce the vibration response and hence reduce brake squeal noise. The design of the constrained layer damping treatment is validated by testing.

INTRODUCTION

Brake squeal is a high frequency, tonal sound generated by the unstable interaction of brake pads on brake disks, or, as in this case, the interaction of brake blocks on steel wheel treads. This phenomenon can be a source of significant noise impacts in terms of both annoyance and sleep disturbance, particularly for residents living beside slow moving rail vehicles undergoing frequent braking. This paper documents the investigation and development of a solution for a rail car brake squeal problem in one such situation.

A diagram of the main elements of the brake system, the brake beam and wheel that are the subject of this paper is shown in Figure 1.

Figure 1 The rail car brake beam and wheel

For the case under consideration, the noise from brakes squealing was dominated by tonal contributions occurring at frequencies around 5kHz, although significant tones were also present at lower frequencies. A very significant reduction in wayside noise levels of approximately 15-20dBA pk was required in order to alleviate noise impacts at the wayside.

Track-side mitigation measures such as noise walls were deemed not to be feasible in this instance due to site operational and maintenance constraints and could not be designed to yield a sufficient noise reduction in any case. A vehicle-based noise mitigation measure was required that would dramatically reduce squeal noise at source.

Potential vehicle-based solutions to this problem include vehicle shrouds as well as brake system and wheel modifications. Shrouds are difficult to implement effectively in practice as they hinder access to the mechanical parts of the vehicle and cannot be sufficiently sealed to generate large enough reductions in noise at the wayside. Brake system and wheel modifications generally require a greater degree of understanding of the squeal phenomenon, which is examined briefly from a theoretical and experimental basis in the following section of this paper.

One of the common problems with investigating squeal-like behaviour is that the squeal response is inherently unstable and is influenced by environmental and operational variables that are difficult if not impossible to control in a test on a vehicle (Triches et al. 2004). Therefore vehicle testing must be approached with caution and an expectation that the results will be variable. Dynamometer tests are preferred for dealing with squeal problems, but these require an investment in specially designed facilities that were not available for the current project. Therefore only full vehicle dynamic tests or stationary assembly-level tests were used in this study.

The friction constant at the brake/wheel interface is a key parameter in determining whether the brake and wheel system will squeal (Chung et al. 2003). Vehicle-level trials were initially conducted using brake blocks with different frictional properties and geometry modified by feathering the leading and trailing edges of the block. Some reductions in squeal noise were achieved, however, within the range of brake blocks that were suitable for long term braking operation, no significant and lasting noise benefit was obtained.

Structural dynamic modification was investigated as a potentially elegant mitigation measure. However, there were problems with this approach due to instabilities in the dominant squeal frequency and therefore a damping treatment, which mitigates vibration and hence noise across a range of frequencies, was proposed as a more robust way forwards.

Interfacial damping such as can be generated by a damping ring inserted into a groove in the wheel can be very effective in reducing high frequency wheel vibration, but it is difficult to model accurately. There may also be issues of deteriorating effectiveness over time due to dust and corrosion. The focus of the noise mitigation exercise was therefore directed towards material-based damping rather than interfacial damping.

THEORETICAL OVERVIEW

Rail Car Brake Squeal

There are a number of documented error states that can occur in brake systems that result in unpleasant noises. Some low frequency noises, known variously as “graunch”, “grunt” and “moan” (Chung et al. 2003), occur at frequencies less than about 1kHz. These noises are generated directly by friction-induced excitation of the brake components, which excites modes in the system.

Brake squeal is a high frequency phenomenon, typically occurring at frequencies above 1kHz and arising from a more complex set of conditions than the low frequency error states described above. Brake squeal is associated with dynamic instability and very high amplitude vibration and acoustic responses radiated by elements in the system.

There may be more than one mechanism leading to brake squeal noises on rolling stock. One of the potential mechanisms is similar to that which causes curve squeal as commonly experienced on track curves of radius less than 300m. This mechanism is “stick-slip”, which arises due to differences in static and dynamic coefficients of friction at the brake-tread interface.

A second mechanism is “sprag-slip”, which results from geometric coupling between the two contacting parts of the brake system, the brake shoe and the wheel in this case. During “sprag-slip”, the contacting parts have mode shapes with similar frequencies and structural wavelengths and they become geometrically and dynamically coupled, leading to a self-excited motion, which is unstable and builds to very high amplitude (Triches et al. 2004).

As a precursor to developing a solution for the rail car brake squeal problem, a systematic investigation was undertaken by instrumenting the brake mechanism of the vehicle with a number of accelerometers in order to describe the natural modes of vibration and operating deflection shapes of the brake system. A modal analysis was also undertaken for the wheel, insitu, while the vehicle was stationary. Finite element models were then developed for both the brake system and the wheel and these were validated using the test data before being used to further interpret the wheel and brake system dynamic behaviour.

The measurement locations on the brake system and wheel are shown in Figure 2a and 2b respectively.

(a)

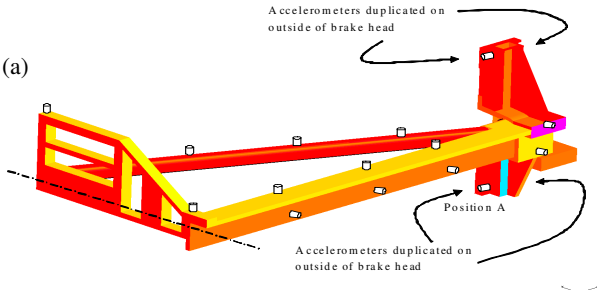

(b)

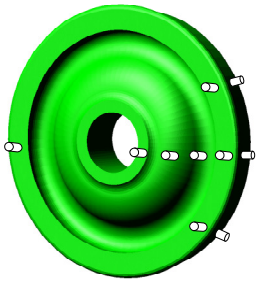

Figure 2 Measurement positions

The relevant 5kHz test and finite element model mode shapes for the brake and wheel are shown in Figure 3a and 3b respectively.

Significantly, the structural wavelengths in the wheel and the brake head shown in Figure 3 are of similar dimension at 5kHz. There is also another similarity in the two mode shapes in that both the tread of the wheel and the brake head undergo significant torsional deformation.

Based on the above observations relating to the wheel and brake mode shapes at the squeal frequency, it appears likely that the squeal mechanism involves geometric coupling between the wheel and brake. If not for the lack of a stable brake squeal frequency, then modifying these mode shapes would likely be a promising approach for remedying the squeal issue. However, given the lack of stability in the dynamic response of the system, a more robust approach, constrained layer damping, was pursued, which is effective across a wide range of frequencies.

(a)

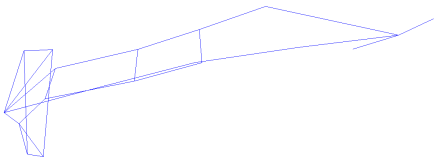

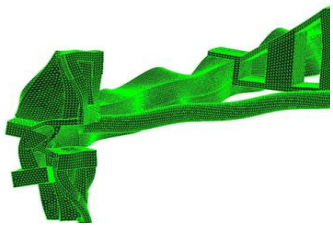

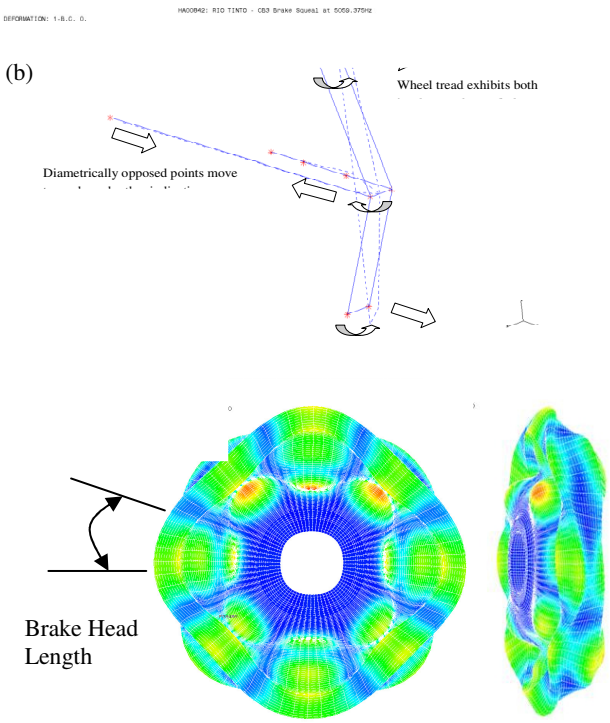

Figure 3 Measured and modelled modes at 5kHz

Constrained Layer Damping

The simplest form of damping involving the addition of a damping layer to a vibrating surface is unconstrained layer damping, where the damping material is simply adhered to the structure. The damping in this arrangement is generated by direct bending strain in the damping material, which can be very effective when the parent structure is thin relative to the damping sheet (Mead 1998). In practice, for steel or aluminium structures of moderate thickness, the damping that can be achieved from an unconstrained layer treatment is limited. This is due to the fact that high loss factor materials tend to have a relatively low modulus and in practical thicknesses (typically 1 to 3 times the substrate thickness), cannot store sufficient strain energy to generate a high composite loss factor (Mead 1998).

A rail wheel typically has a relatively thick web and an even more substantial tread cross-section. The web for the wheel under consideration has a minimum thickness of 28mm and it is not feasible to provide sufficiently high levels of damping using unconstrained layer damping in this scenario. Figure 4 shows the wheel cross-section.

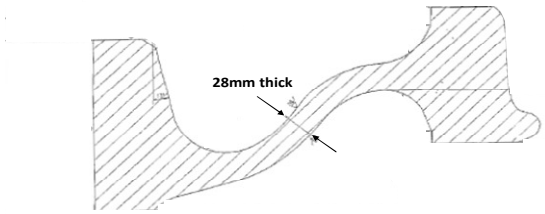

Figure 4 Wheel cross-section

A more effective alternative to unconstrained layer damping in this situation is constrained layer damping (CLD). CLD works by adding a constraining layer of relatively stiff material to the outside of a viscoelastic damping layer so that damping losses are generated by the shear strain in the damping layer. Figure 5 shows the CLD configuration. The main advantage of this compared with unconstrained layer damping is that the maximum loss factor of the composite system is no longer dependent solely on increasing the thickness of the damping layer. Very high composite loss factors can be generated using very small quantities of damping material and an optimum configuration exists, which is a function of the damping material modulus, loss factor and thickness as well as the wavelengths of structural vibration in the parent and constraining plates (Mead 1998).

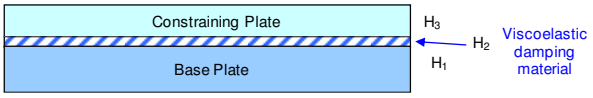

Figure 5 **Constrained layer damping configuration**

The general performance characteristics of CLD applications are described in (Beranek et al. 1992), with the combined loss factor (η) for the base plate, viscoelastic material interlayer and the constraining plate being described by;

$$\eta = \frac{\beta Y X}{1+(2+Y)X+(1+Y)(1+\beta^2)X^2} \qquad 1$$

where the Shear Parameter (*X*) and the Structural Parameter (*Y*) are represented by

$$X = \frac{G_2}{p^2 H_2} S \qquad \frac{1}{Y} = \frac{E_1 H_1^3 + E_3 H_3^3}{12 H_{31}^2} S \qquad 2$$

$$S = \frac{1}{E_1 H_1} + \frac{1}{E_3 H_3} \qquad 3$$

β = Loss factor of viscoelastic material

G_2 = Shear modulus of viscoelastic material

E_i = Elastic modulus of i^{th} layer

H_i = Thickness of i^{th} layer

H_{13} = Distance between neutral axis of base plate and constraining plate

p = Wavenumber ($2\pi/\lambda$)

It can be shown that the combined loss factor (η) of the CLD system will be maximised when the Shear Parameter (X) is at an optimum (X_{opt});

$$X_{opt} = \frac{1}{\sqrt{(1+Y)(1+\beta^2)}} \qquad 4$$

Several key trends in CLD performance are presented in Figure 6 based on the theoretical method above. The upper plot illustrates how the composite loss factor decreases with a reduction in constraining plate thickness, where the base plate thickness is 50 mm the damping material is 3.2 mm thick and the constraining layer varies from 5 to 25 mm. Note how the frequency of maximum performance remains unchanged. The optimum loss factor is achieved when the constraining layer approaches the base layer thickness. The lower plot of Figure 6 illustrates the effect of reducing the inter-layer damping material thickness for a constant constraining layer thickness. Reducing the damping layer thickness to one third of the initial value is observed to raise the frequency of peak performance by nominally one decade.

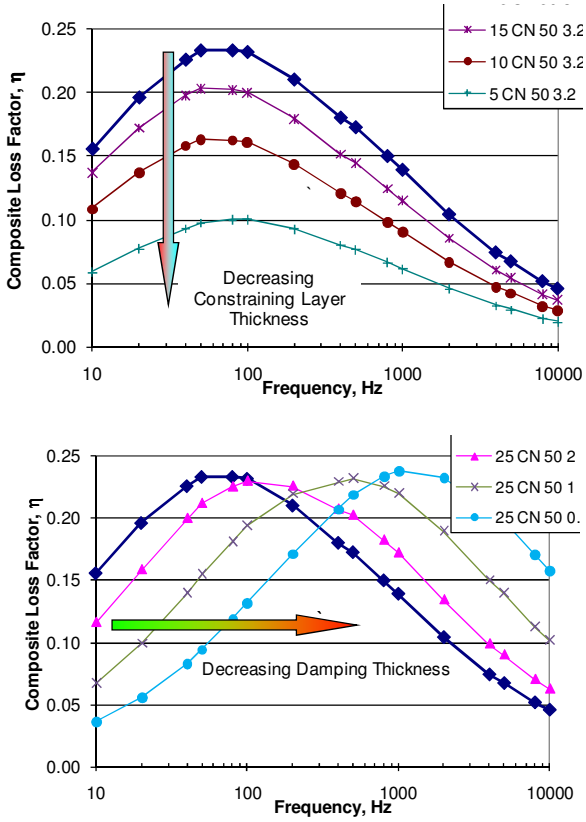

Figure 6 Composite loss factor of CLD treatments for varying constraining layer thickness (upper) and damping material thickness (lower).

A common failing of CLD systems to realise their maximum potential is that the elastic modulus of the damping layer is not "matched' to the bending stiffness of the base and constraining layer. Figure 7 illustrates the effect of utilising a damping material that is too flexible for the thick plate application of 28 mm base plate thickness, 3.2 mm damping material and 16 mm steel constraining layer. The CN damping material has an elastic modulus that is approximately 6 to 10 times stiffer throughout the 10 Hz to 10 kHz frequency regime compared to the softer C1100 material. Despite the fact that the C1100 material has a higher loss factor (0.65 – 1.0) than the CN material (0.7 – 0.8), for the same thickness distribution the C1100 performs poorly for all frequencies > 60 Hz.

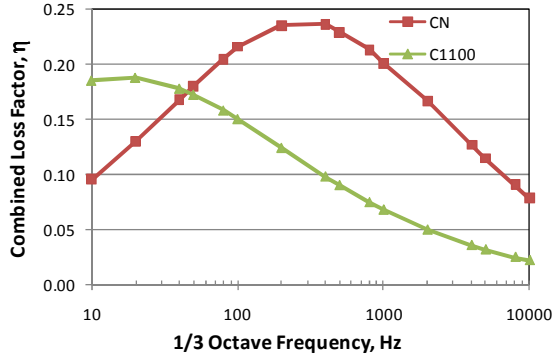

Figure 7 composite loss factors of CLD Treatments for varying damping material stiffness

THE DESIGN OF THE CONSTRAINED LAYER DAMPING TREATMENT

The procedure for systematically designing CLD is iterative and there are several steps involved. In the present case the design approach was divided into two stages, each with its own set of sub tasks. The first stage involved the design of a CLD treatment for the ideal case of a pair of thick circular constraining plates in a free-free configuration with an intervening damping layer. This was carried out using aspects of the theoretical approach described in detail by (Mead 1998). The second stage of the design involved the use of a finite element model (FEM). The FEM was first validated using the newly created theoretical model of the 28mm thick plates. The same finite element modelling approach was then used to model the wheel acting together with the CLD treatment in order to refine the damper design.

The steps involved in the first stage of the CLD design process are described briefly below. In practice, the theoretical approach of (Mead 1998) is altered to reflect available material properties and material thicknesses. Under these conditions the CLD equations become step functions rather than smooth functions and it is appropriate to set practical constraints on the problem based on known available material configurations and available package space.

The starting point for the CLD design process remains the selection of candidate damping materials that have high loss factors over the temperature range of interest. These damping materials are available in a small selection of discrete thicknesses and so it makes sense to select the damping sheet thickness and keep this constant whilst varying the constraining layer thicknesses to achieve an optimum damping outcome.

In this case the optimisation calculations were performed using a linear optimisation routine with the objective of maximising the composite damping level over the 1 – 4kHz octave band range. The outcome of the calculation procedure was the optimum constraining plate thickness for a given damping sheet thickness and loss factor at operating temperature.

Based on the modelling procedure described above, a relatively stiff damping material, "CN damping sheet", was selected. This material is available in a limited range of thicknesses and so the 3.2mm thick damping material layer that was selected reflects this design constraint. If a thinner CN damping layer were to be available, this would be beneficial to the performance of the design.

The performance of a 3.2mm thick layer of CN damping sheet and two 28mm thick constraining plates provided was defined using the previously described theoretical calculation procedure. The predicted composite damping loss factor was approximately 0.074 compared to a loss factor of about 0.002 for the parent steel plate.

The FEM of the idealised damper arrangement is shown in Figure 8. The IDEAS finite element software package was used to model the system using eight-noded brick elements to model the two steel disks and the damping layer. The steel disks were two elements thick, while the damping layer was modelled using three elements through the thickness.

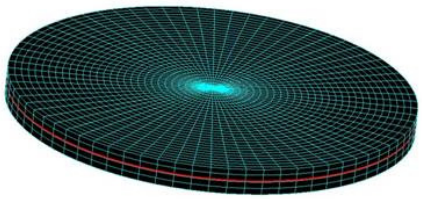

Figure 8 Finite element model (FEM) of the idealised constrained layer damping configuration

Material-based damping was input to the model in the form of a loss factor proportional to the distributed stiffness. This

results in a complex stiffness matrix. If the model had only one material type, an equivalent modal viscous damping ratio could be calculated in a straight-forward manner and applied at the resonant frequencies in order to represent the damping behaviour in the system. Modal domain techniques could then easily be applied to analyse the model. Because there are two materials with radically different damping properties in the system, non-proportional damping exists. That is, the overall damping is not proportional to the mass or stiffness matrices. This means that the system mass and stiffness matrices cannot be diagonalised using modal coordinates for the combined steel plate and damping material model and so straight-forward modal-domain techniques cannot be used to determine the combined loss factor for the CLD system. It is possible that a substructuring approach could be used to develop separate models of the steel plates and damping layer in the modal domain, which could then be combined. A more computationally expensive, but ultimately expedient way of proceeding is to use the direct frequency response method. This involves directly solving the complex forced response equation below with fully populated matrices:

$$[M]\{\ddot{x}\}+[K+Ki]\{x\}=\{F\} \qquad 5$$

The driving point response of the idealised CLD system for an out-of-plane force acting at the circumference of one of the disks was calculated using the finite element model. The combined loss factor in the system may be estimated using the half power point method at the resonant peaks.

The combined system loss factor from the FEM shown in Figure 8, estimated using the half power point method, is 0.065, which compares favourably with the value of 0.074 calulated using the theoretical model of (Mead 1998). Further successful model validation tests were carried out by varying the constraining plate thickness and comparing the resultant damping loss factors to the FEM results in order to establish confidence in the FEM technique.

Having validated the FEM approach and established a baseline design configuration for the CLD treatment, the CLD model was appended to the finite element model of the wheel as shown in Figure 9. As the intention was to bolt the damping treatment to the rim, less than full connectivity was assumed between the inner plate and the rim. Nodes within about 2 bolt diameters of the centre point of each bolt on the surfaces of the rim and the inner plate were merged.

Figure 9 FEM of wheel with baseline CLD treatment

A number of design iterations were carried out using the FEM shown in Figure 9 to optimise the design and the overall CLD thickness was reduced to be less than 30mm. Due to the CLD design being rationalised to meet practical dimensional requirements an additional design element, a thick steel ring, was used to enhance the damping performance by absorbing energy associated with the rotation of the wheel tread. The final design of the CLD treatment is presented in an exploded view format in Figure 10.

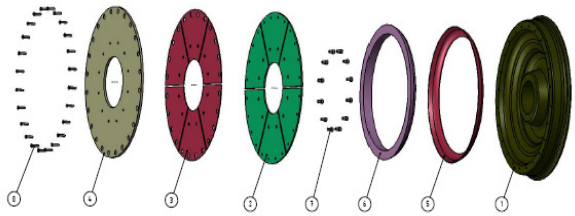

Figure 10 Exploded view of the final CLD design

The predicted damping performance of the combined wheel and CLD system due to radial and axial input forces is given in Figure 11 and 12 respectively. These plots indicate that broad-based energy reduction is to be expected from the system, with a minimum performance of about 16dB at around 5kHz for an axial input and about 10dB for a radial input.

The predicted damping levels for the final design were close to the estimated requirements for the project and so prototype wheel and damper systems were fabricated for a validation test.

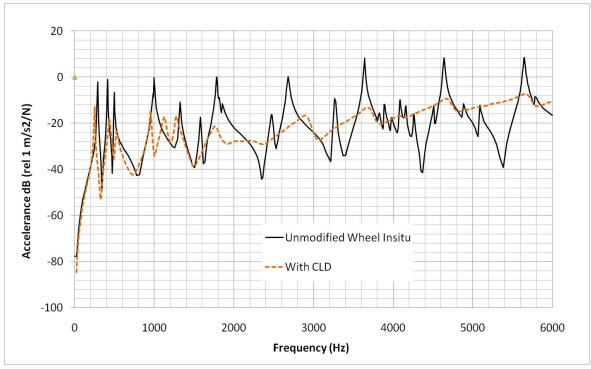

Figure 11 Predicted damping performance of the CLD and wheel system for an axial force

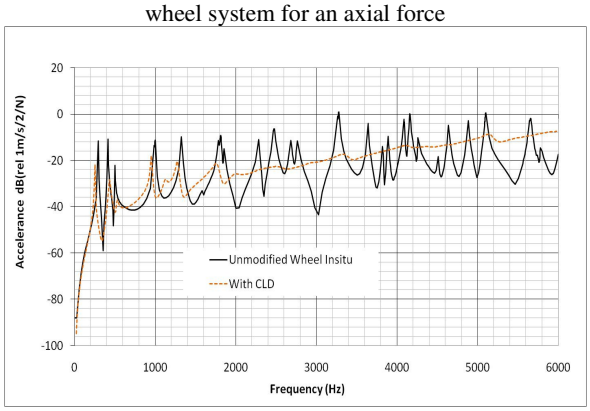

Figure 12 Predicted damping performance of the CLD and wheel system for a radial force

Experimental Validation of the Constrained Layer Damping Performance

In order to validate the design of the CLD treatment for the wheel, an assembly-level validation test was performed. This facilitated a comparison between the predicted damping performance of the treatment and the measured performance. The experimental setup involved impact testing on 2 wheels, one in an unaltered state and one with the CLD treatment comprising the constraining plates, damping sheet and infill ring.

A modal analysis was carried out on the wheel with the full damping treatment, while radial and axial driving point FRFs were obtained on the rim of the unaltered wheel purely to establish the overall difference in damping levels between the two wheels.

The wheels weighed approximately 450kg each and therefore could not be handled manually. Care needed to be taken to support them in a way that did not alter the modes or add to the measured damping levels. This was achieved by placing each wheel horizontally onto a neoprene bearing ring directly supporting the hub and without contacting the web or rim. With mechanical assistance the wheels could then be turned over to facilitate measurements on both sides.

For the modal test on the wheel with the full CLD treatment, a small triaxial accelerometer was positioned on the rim using an epoxy adhesive and an impact hammer was roved across a matrix of measurement positions on a 90 degree arc of the constraining plate and rim. A limited number of measurements were taken on the web and on the diagonally opposite side of the wheel to establish whether the modes were symmetric or anti-symmetric. Figure 13 shows the impact modal test layout on the wheel with the CLD treatment.

Figure 13 Impact modal test layout, showing measurement grid on the constrained layer and reference accelerometer location shown.

Figures 14 - 16 show modal responses at frequencies of interest for the wheel with the full CLD treatment.

Figures 17 and 18 show the driving point FRFs for the two wheel configurations for the radial and axial inputs respectively. Based on these measurement results, the damping levels in the wheel with the CLD treatment indicate an overall loss factor of about 0.02 at 5kHz. Compared to the undamped wheel in a free-free configuration, the reduction in the response due to the CLD treatment is approximately 40dB.

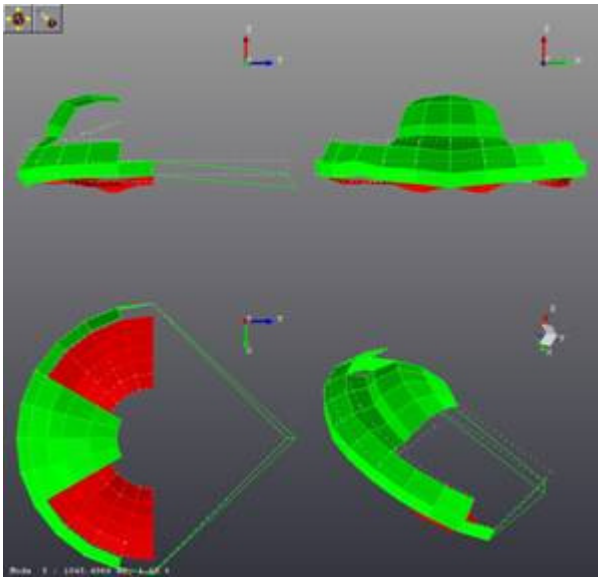

Figure 14 Wheel mode at 1045Hz (1 node along radius, no nodes around circumference)

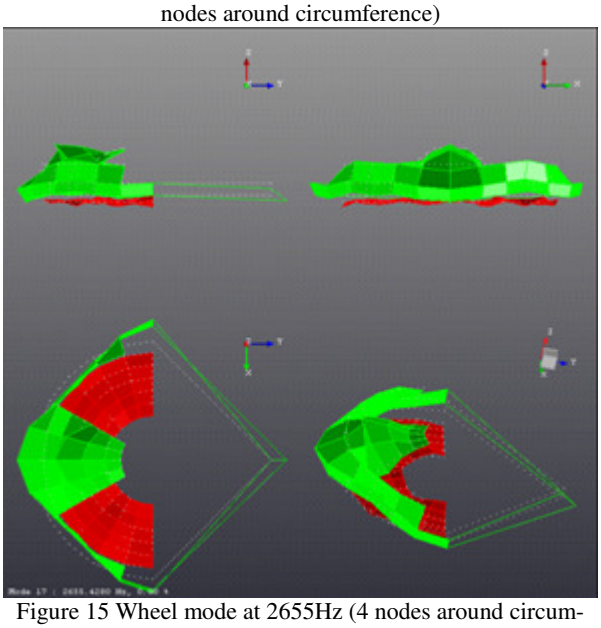

Figure 15 Wheel mode at 2655Hz (4 nodes around circumference, 2 nodes along radius)

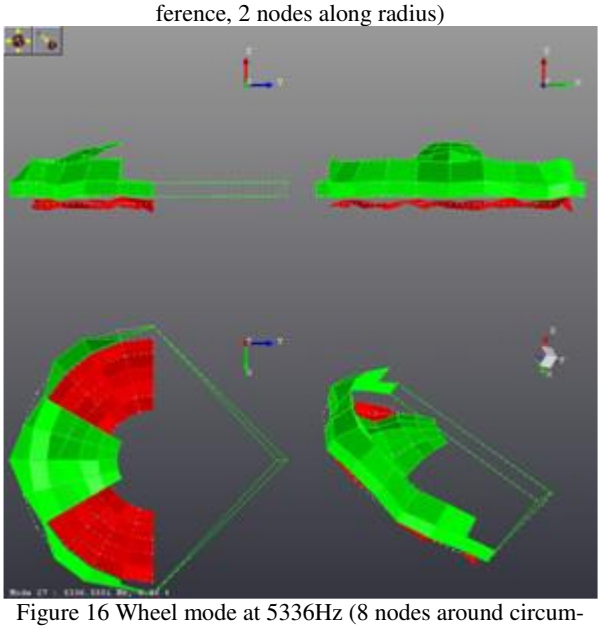

Figure 16 Wheel mode at 5336Hz (8 nodes around circumference, 3 nodes along radius)

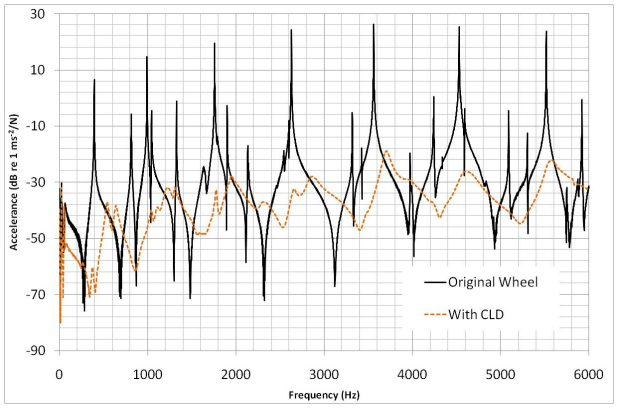

Figure 17 Comparison of driving point axial FRFs; original wheel (solid line) and with CLD treatment (dashed line)

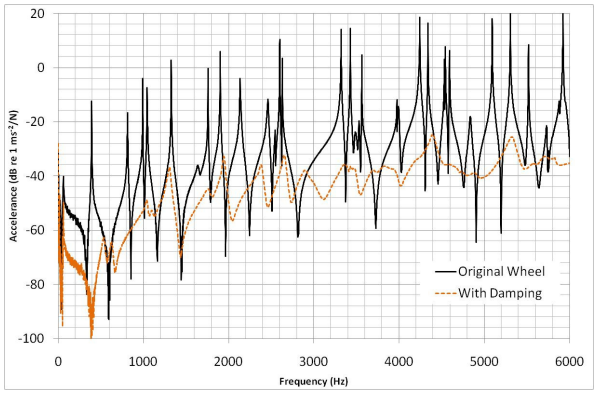

Figure 18 Comparison of driving point radial FRFs; original wheel (solid line) and CLD treatment (dashed line)

DISCUSSION

Brake squeal is a highly non-linear phenomenon and the propensity to squeal and the resultant noise level are highly dependent on minor changes in operating and environmental variables such as temperature, the coefficient of friction, dust, brake pressure and vehicle speed. It is critical in situations such as this to adopt a systematic approach, to spend adequate time to diagnose and understand the problem and to pay careful attention to the effect of measurement variability, particularly in the field on vehicle-level tests. Simulation and component/assembly-level validation testing are therefore key techniques to use in this situation.

In this paper an overview was presented of a systematic investigation and design process in relation to a rail vehicle brake squeal issue. Testing and simulation techniques were used to gain diagnostic data relating to the brake squeal event and the vibro-acoustic properties of the components in the system. Simple theoretical and finite element models were used to design a constrained layer damping treatment to act on the wheels of the rail vehicle and a prototype design was fabricated and tested. The assembly-level validation test showed that the CLD treatment performed well in relation to design expectations.

The test results indicated a better than expected increase in damping levels for the treated wheel compared with the predicted improvement. This is likely to be mostly due to the differences in boundary conditions between the damping measured on the unaltered wheel insitu (as used in the design FEM) and the damping measured on an unaltered wheel in the free-free condition (as in the validation experiment). This apparent performance improvement is not likely to be fully realised on the vehicle due to the presence of rolling damping already in the system, however, the results are very encouraging and indicate that the design has a high probability of working in a field trial.

Further work could be undertaken to develop a theoretical model of the brake squeal event for this application. Such a model may yield a more elegant solution than the one documented in this paper.

REFERENCES

Chung C.H.J., Steed W., Dong J., Kim B.S. and G.S. Ryu, (2003) “Virtual design of brake squeal”, SAE 2003-01-1625

Misra H., Nack W., Kowalski T., Komzsik L. and Johnson E., (1999) “Brake analysis and NVH optimisation using MSC Nastran”, 1st Worldwide MSC Automotive Users Conference, Sept 20-22, 1999.

Triches M. Jr., Gerges S.N.Y. and Jordan R., (2004) “Reduction of squeal noise from disc brake systems using constrained layer damping”, The Journal of the Brazilian Society of Mechanical Science and Engineering, July-Sept 2004, Vol XXVI, No 3.

Mead D.J., (1998) *Passive Vibration Control*, John Wiley & Sons.

Beranek L.L, Ver I.L, (1992) "Noise & Vibration Control Engineering" John Wiley & Sons, pp 477-450